IJST, Transactions of Civil Engineering, Vol. 39, No. C1, pp 21-40
Printed in The Islamic Republic of Iran, 2015

OPTIMUM PARAMETERS OF TUNED MASS DAMPERS FOR SEISMIC APPLICATIONS USING CHARGED SYSTEM SEARCH*

A. KAVEH[1**], S. MOHAMMADI[2], O. KHADEM HOSSEINI[3], A. KEYHANI[4] AND V.R. KALATJARI[5]

[1]Centre of Excellence for Fundamental Studies in Structural Engineering,
Iran University of Science and Technology, Narmak, Tehran-16, I. R. of Iran
Email: alikaveh@iust.ac.ir
[2-5]Dept. of Civil and Architectural Engineering, University of Shahrood, Shahrood, I. R. of Iran

Abstract– In this paper, optimum parameters of Tuned Mass Dampers (TMD) are determined to minimize the dynamic response of multi-story building systems under seismic excitations. Charged System Search (CSS), as an efficient optimization algorithm, is revised and applied for tuning passive mass dampers. A MATLAB program is developed for numerical optimization and time domain simulation. Optimization criteria are the peak values of the first story displacement with and without TMD, and the transfer function from input ground acceleration to the first story acceleration response. An alternative formulation is also presented for solving state space equations. Compared to other population-based meta-heuristics, the charged system search has a number of advantages distinguishing this algorithm from the others. However, for improving exploitation (the fine search around a local optimum), it is hybridized with HS that utilizes charged memory (CM) to speed up its convergence. To ensure good performance of this approach, some numerical considerations are conducted to verify the effectiveness and feasibility of the presented approach.

Keywords– Tuned mass damper, charged system search, structural control, state space equations of motion

1. INTRODUCTION

In the history of structural engineering, a number of methods have been developed and adopted for vibration control in order to reduce the structural response due to lateral excitations. The methodologies utilized to improve the structural performance and to minimize the structural damage, consist of vibration isolation, control of excitation forces, vibration absorber, etc. In the case of vibration absorbers, Tuned Mass Damper (TMD), Active Mass Damper (AMD), and Hybrid Mass Damper (HBD) have been utilized to control the behavior of tall structure subjected to excitations. Among these systems, TMD is the most popular one due to its simple principle and several successful applications in real life practice. TMD is a passive control system consisting of mechanical components such as mass, springs and viscous dampers which assists to increase the damping of the primary structure and hence aids in reducing vibration and keeping it within the desirable limits.

The concept of vibration control, using a mass damper, dates back to the year 1909 when Frahm [1] proposed the basic form of TMD which did not possess any damping property by itself. After that Ormondroyd and Den Hartog [2] introduced internal damping in TMDs. Further investigations were carried out on TMDs effectiveness in reducing the response of structures subjected to harmonic [3] and wind [4, 5] excitations.

The design of TMDs involves selection of three parameters: mass, damping and stiffness. Optimum values of these parameters were considered by Den Hartog [3] for the first time, where the harmonic

*Received by the editors January 15, 2014; Accepted June 28, 2014.
**Corresponding author

loading was applied to an undamped single degree of freedom system (SDOF) system. Later, damping in the main system was included through several researches by Falcon et al. [6], Warburton [7].

Further investigations have been carried out by Sadek et al. [8] considering practical considerations. Hadi and Arfiadi [9] used the genetic algorithm to optimize the TMD parameters. In this work the H_2 norm of the transfer function from the external disturbance to a regulated output was taken as a performance measure of the optimization criterion. Lee et al. [10] proposed a numerical method to estimate optimum parameters of TMD. They used power spectral density function of external disturbance, in return external and optimization process was performed based on minimizing the performance index of structural responses defined in the frequency domain. In another study, harmony search algorithm was empoyed as an optimization technique [11]. In their study, optimum TMD parameters were estimated assuming harmonic loading subjected to the structure. The result of their work showed very good reduction in structural responses, however, these results are yet under discussion [12, 13].

Due to the complexity of parameters involved in structures, it is necessary to use a practical approach such as numerical optimization method. In the last decade, many new natural evolutionary algorithms have been developed for optimization of engineering problems, such as genetic algorithms (GAs) [14], particle swarm optimizer (PSO) [15], ant colony optimization (ACO) [16] and harmony search (HS) [17], charged system search (CSS) [18–19]. These methods have attracted a great deal of attention, because of their high potential for modeling engineering problems in environments which have been resistant to solution by classic techniques. They do not require gradient information and possess better global search abilities than the conventional optimization algorithms. Having in common processes of natural evolution, these algorithms share many similarities: each maintains a population of solutions which are evolved through random alterations and selection. The differences between these procedures lie in the representation technique utilized to encode the candidates, the type of alterations used to create new solutions, and the mechanism employed for selecting new patterns.

Meta-heuristic algorithms have been widely used for the optimization of TMD parameters. The meta-heuristic methods used for the optimization are genetic algorithm [20–21], bionic algorithm [22], particle swarm optimization [23], harmony search method [11, 24-26], ant colony optimization [27] and evolutionary operation [28].

2. EQUATIONS OF MOTION

Consider an N-story shear building structure with mass damper installed at the top floor as shown in Fig. 1. The equation of motion of the structural system can be written as:

$$\mathbf{M}\,\ddot{\mathbf{X}}(t)+\mathbf{C}\,\dot{\mathbf{X}}(t)+\mathbf{K}\,\mathbf{X}(t)=\mathbf{F}(t) \tag{1}$$

where $\mathbf{M,\ C,\ K}$ are mass, damping, and stiffness matrices with the formulations below:

$$\mathbf{M}=diag\begin{bmatrix} m_1 & m_2 & \cdots & m_{N-1} & m_N \end{bmatrix} \tag{2}$$

$$\mathbf{C}=\begin{bmatrix} (c_1+c_2) & -c_2 & & & & & \\ -c_2 & (c_2+c_3) & -c_3 & & & & \\ & \ddots & \ddots & \ddots & & & \\ & & & \ddots & \ddots & & \\ & & & & \ddots & \ddots & \\ & & & & -c_N & (c_N+c_d) & -c_d \\ & & & & & -c_d & -c_d \end{bmatrix} \tag{3}$$

$$\mathbf{K}=\begin{bmatrix} (k_1+k_2) & -k_2 & & & & & \\ -k_2 & (k_2+k_3) & -k_3 & & & & \\ & \ddots & \ddots & \ddots & & & \\ & & & \ddots & \ddots & & \\ & & & & -k_N & (k_N+k_d) & -k_d \\ & & & & & -k_d & -k_d \end{bmatrix} \tag{4}$$

$$\mathbf{X}=\begin{bmatrix} x_1 & x_2 & \cdots & x_N & x_d \end{bmatrix}^T \tag{5}$$

$$\mathbf{F}=\begin{bmatrix} f_1 & f_2 & \cdots & f_N & f_d \end{bmatrix}^T \tag{6}$$

Where m_i is the mass of the ith floor $(i=1,\ 2,\ \cdots,\ N)$; m_d is the mass of the damper; c_i is the damping of the ith floor $(i=1,\ 2,\ \cdots,\ N)$; c_d is the damping of the damper; k_i is the stiffness of the ith floor $(i=1,\ 2,\ \cdots,\ N)$; k_d is the stiffness of the damper; x_i is the displacement of the ith floor relative to ground $(i=1,\ 2,\ \cdots,\ N)$; x_d is the displacement of damper relative to ground; f_i is the external force applied at ith floor $(i=1,\ 2,\ \cdots,\ N)$; f_d is the external force applied at the absorber. A schematic model is shown in Fig. 1.

The equation of motion can be converted to state-space equation as

$$\dot{\mathbf{Z}}(t)=\mathbf{A}\mathbf{Z}(t)+\mathbf{B}\mathbf{F}(t) \tag{7}$$

$$\mathbf{Y}(t)=\mathbf{R}\mathbf{Z}(t)+\mathbf{Q}\mathbf{F}(t) \tag{8}$$

Where:

$$\mathbf{Z}(t)=\begin{Bmatrix} \mathbf{X}(t) \\ \dot{\mathbf{X}}(t) \end{Bmatrix} \tag{9}$$

$$\mathbf{A}=\begin{bmatrix} [\mathbf{0}]_{(N+1)\times(N+1)} & [\mathbf{I}]_{(N+1)\times(N+1)} \\ -\mathbf{M}^{-1}\mathbf{K} & -\mathbf{M}^{-1}\mathbf{C} \end{bmatrix} \tag{10}$$

$$\mathbf{B}=\begin{bmatrix} [\mathbf{0}]_{(N+1)\times(N+1)} \\ \mathbf{M}^{-1} \end{bmatrix} \tag{11}$$

$\mathbf{I}$ is the identity matrix, and $\mathbf{R}$ and $\mathbf{Q}$ are the system matrices where based on the type of the regulated output $\mathbf{Y}$. Note that the regulated output in Eq. (8) can be taken as displacement, velocity, or acceleration. In this paper, we use displacement and acceleration as regulated outputs; in the case when the regulated output is taken as the relative displacement of floors and TMD with respect to the ground, the matrices $\mathbf{R}$ and $\mathbf{Q}$ can be written as:

$$\mathbf{R}=\begin{bmatrix} [\mathbf{I}]_{(N+1)\times(N+1)} & [\mathbf{0}]_{(N+1)\times(N+1)} \end{bmatrix},\ \mathbf{Q}=[\mathbf{0}]_{(N+1)\times(N+1)} \tag{12}$$

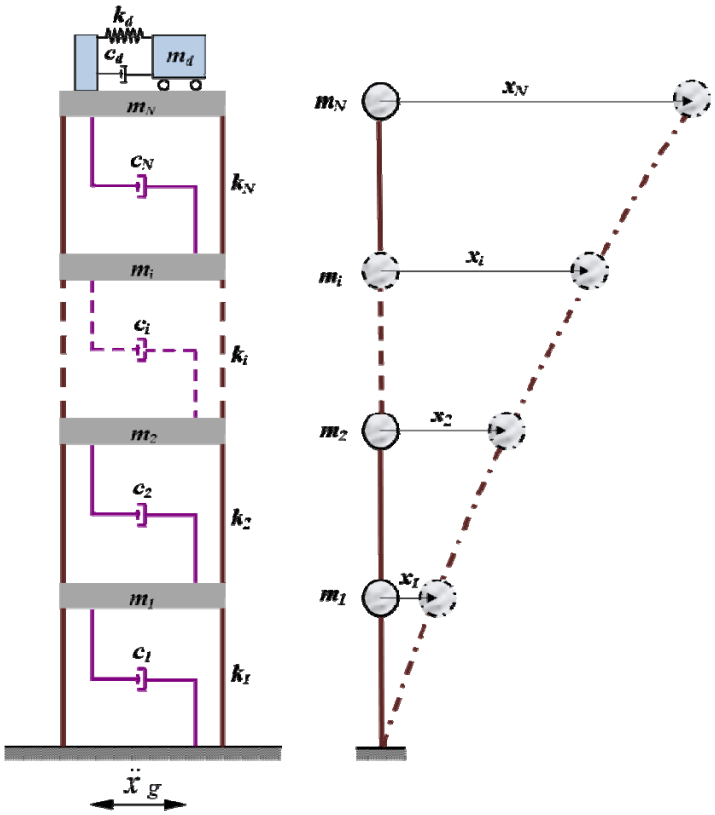

Fig. 1. Schematic model of a multi-story shear building structure with single TMD

Alternatively if the regulated output is taken as the absolute acceleration of the floors and TMD, the matrices $\mathbf{R}$ and $\mathbf{Q}$ can be written as:

$$\mathbf{R} = \begin{bmatrix} -\mathbf{M}^{-1}\mathbf{K} & -\mathbf{M}^{-1}\mathbf{C} \end{bmatrix}, \quad \mathbf{Q} = [\mathbf{M}^{-1}] \tag{13}$$

It should be noted that if the external loading is the base acceleration (earthquake loading), vector $\mathbf{F}$ can be defined as:

$$\mathbf{F}(t) = -\mathbf{M}\{1\}_{(N+1)\times 1}\ddot{x}_g(t) \tag{14}$$

a) Solution of the state space differential equation

In this paper, matrix exponential approach [29] is utilized to solve the aforementioned state space differential equation. Let us return to Eq. (7) and begin by guessing a solution of the form $\mathbf{Z}(t) = e^{\mathbf{A}t}\mathbf{v}(t)$, where $\mathbf{v}(t)$ is a time-varying vector. Differentiating the solution results in:

$$\frac{d\mathbf{Z}(t)}{dt} = \mathbf{A}e^{\mathbf{A}t}\mathbf{v}(t) + e^{\mathbf{A}t}\frac{d\mathbf{v}(t)}{dt} \tag{15}$$

In the other hand, replacing the solution in Eq. (7) we get:

$$\frac{d\mathbf{Z}(t)}{dt} = \mathbf{A}e^{\mathbf{A}t}\mathbf{v}(t) + \mathbf{B}\mathbf{F}(t) \tag{16}$$

Comparing Eqs. (15) and (16) results in:

$$e^{\mathbf{A}t}\frac{d\mathbf{v}(t)}{dt}=\mathbf{B}\mathbf{F}(t) \tag{17}$$

Or

$$\frac{d\mathbf{v}(t)}{dt}=e^{-\mathbf{A}t}\mathbf{B}\mathbf{F}(t) \tag{18}$$

Solving this by integration, we obtain:

$$\mathbf{v}(t)-\mathbf{v}(t_0)=\int_{t_0}^{t}e^{-\mathbf{A}\tau}\mathbf{B}\mathbf{F}(\tau)d\tau \tag{19}$$

Since $\mathbf{v}(t)=e^{-At}\mathbf{Z}(t)$ and $\mathbf{v}(t_0)=e^{-\mathbf{A}t_0}\mathbf{Z}(t_0)$, then:

$$e^{-\mathbf{A}t}\mathbf{Z}(t)-e^{-\mathbf{A}t_0}\mathbf{Z}(t_0)=\int_{t_0}^{t}e^{-\mathbf{A}\tau}\mathbf{B}\mathbf{F}(\tau)d\tau \tag{20}$$

Therefore analytical solution of Eq. (7) can be obtained by matrix exponential approach as:

$$\mathbf{Z}(t)=e^{\mathbf{A}(t-t_0)}\mathbf{Z}(t_0)+e^{\mathbf{A}t}\int_{t_0}^{t}e^{-\mathbf{A}\tau}\mathbf{B}\mathbf{F}(\tau)d\tau \tag{21}$$

To derive the discrete form of the above solution, over the ith interval letting $t=(i+1)T$ and $t_0=iT$, we have:

$$\mathbf{Z}_{i+1}=e^{\mathbf{A}T}\mathbf{Z}_i+\int_{iT}^{(i+1)T}e^{\mathbf{A}[(i+1)T-\tau]}\mathbf{B}\mathbf{F}(\tau)d\tau \tag{22}$$

Where T is the sampling period. Now introducing a new variable η as $\eta=\tau-iT$, we obtain:

$$d\eta=d\tau;\ (i+1)T-\tau=T-\tau \tag{23}$$

On the other hand, if sampling period is sufficiently small, then $\mathbf{F}(t)$ can be written as a piecewise constant function over the ith time interval:

$$\mathbf{F}(t)=\mathbf{F}_i,\ iT\le t\le(i+1)T \tag{24}$$

Now we have:

$$\mathbf{Z}_{i+1}=e^{\mathbf{A}T}\mathbf{Z}_i+\left[\int_0^T e^{\mathbf{A}(T-\eta)}d\eta\right]\mathbf{B}\mathbf{F}_i \tag{25}$$

And then:

$$\mathbf{Z}_{i+1}=e^{\mathbf{A}T}\mathbf{Z}_i+e^{\mathbf{A}T}\left[-\mathbf{A}^{-1}e^{-\mathbf{A}\eta}\right]_0^T\mathbf{B}\mathbf{F}_i \tag{26}$$

Therefore, the final result is obtained as:

$$\mathbf{Z}_{i+1}=e^{\mathbf{A}T}\mathbf{Z}_i+\mathbf{A}^{-1}\left(e^{\mathbf{A}T}-\mathbf{I}\right)\mathbf{B}\mathbf{F}_i \tag{27}$$

The presented formulation finds only the structural response to external excitation at each step, and it has no effect on the original optimization problem.

3. THE STANDARD CSS

Recently an efficient optimization algorithm, known as the charged system search, is developed by Kaveh and Talatahari [18]. This algorithm is based on the laws from electrostatics and Newtonian mechanics.

The Coulomb and Gauss laws provide the magnitude of the electric field at a point inside and outside a charged insulating solid sphere, respectively, as follows [18]:

$$\begin{cases} \vec{\mathbf{E}}_{ij} = k_e \dfrac{q_i}{\vec{\mathbf{r}}_{ij}^2} & : \vec{\mathbf{r}}_{ij} \geq a \\ \vec{\mathbf{E}}_{ij} = k_e \dfrac{q_i}{a^3} \vec{\mathbf{r}}_{ij} & : \vec{\mathbf{r}}_{ij} < a \end{cases} \tag{28}$$

where k_e is a constant known as the Coulomb constant; $\vec{\mathbf{r}}_{ij}$ is the separation of the centre of sphere and the selected point; q_i is the magnitude of the charge; and "a" is the radius of the charged sphere. Using the principle of superposition, the resulting electric force due to *N* charged spheres is equal to [18]:

$$\vec{\mathbf{F}}_{ij} = k_e q_j \sum_{i,i \neq j} \left(\frac{q_i}{a^3} \vec{\mathbf{r}}_{ij} . i_1 + \frac{q_i}{\vec{\mathbf{r}}_{ij}^2} . i_2 \right) \frac{\vec{\mathbf{r}}_i - \vec{\mathbf{r}}_j}{\left\| \vec{\mathbf{r}}_i - \vec{\mathbf{r}}_j \right\|} \qquad \begin{cases} i_1 = 1, i_2 = 0 \Leftrightarrow \vec{\mathbf{r}}_{ij} < a \\ i_1 = 0, i_2 = 1 \Leftrightarrow \vec{\mathbf{r}}_{ij} \geq a \end{cases} \tag{29}$$

Also, according to the Newtonian mechanics, we have:

$$\begin{cases} \Delta \vec{\mathbf{r}} = \vec{\mathbf{r}}_{new} - \vec{\mathbf{r}}_{old} \\ \vec{\mathbf{v}} = \dfrac{\vec{\mathbf{r}}_{new} - \vec{\mathbf{r}}_{old}}{t_{new} - t_{old}} = \dfrac{\vec{\mathbf{r}}_{new} - \vec{\mathbf{r}}_{old}}{\Delta t} \\ \vec{\mathbf{a}} = \dfrac{\vec{\mathbf{v}}_{new} - \vec{\mathbf{v}}_{old}}{\Delta t} \end{cases} \tag{30}$$

where $\vec{\mathbf{r}}_{old}$ and $\vec{\mathbf{r}}_{new}$ are the initial and final positions of the particle, respectively; $\vec{\mathbf{v}}$ is the velocity of the particle; and $\vec{\mathbf{a}}$ is the acceleration of the particle. Combining the above equations and using the Newton's second law, the displacement of any object as a function of time is obtained as:

$$\vec{\mathbf{r}}_{new} = \frac{1}{2} \frac{\vec{\mathbf{F}}}{m} . \Delta t^2 + \vec{\mathbf{v}}_{old} . \Delta t + \vec{\mathbf{r}}_{old} \tag{31}$$

Inspired by the above electrostatic and Newtonian mechanics laws, the pseudo-code of the CSS algorithm is presented as follows [18]:

*Level 1**: Initialization***

Step 1. Initialization. Initialize the parameters of the CSS algorithm. Create an array of charged particles (CPs) with random positions. The initial velocities of the CPs are taken as zero. Each CP has a charge of magnitude (q_i) defined by considering the quality of its solution as:

$$q_i = \frac{fit(i) - fit_{worst}}{fit_{best} - fit_{worst}} \quad , i = 1, 2, ..., N \tag{32}$$

where fit_{best} and fit_{worst} are the best and the worst fitness of all the particles; $fit(i)$ represents the fitness of agent *i*. The separation distance r_{ij} between two charged particles is defined as:

$$\vec{\mathbf{r}}_{ij} = \frac{\left\| \vec{\mathbf{X}}_i - \vec{\mathbf{X}}_j \right\|}{\left\| (\vec{\mathbf{X}}_i + \vec{\mathbf{X}}_j)/2 - \vec{\mathbf{X}}_{best} \right\| + \varepsilon} \tag{33}$$

where $\vec{\mathbf{X}}_i$ and $\vec{\mathbf{X}}_j$ are the positions of the *i*th and *j*th CPs, respectively; $\vec{\mathbf{X}}_{best}$ is the position of the best current CP; and ε is a small positive to avoid singularities.

Step 2. CP ranking. Evaluate the values of the fitness function for the CPs, compare them with each other and sort them in increasing order.

Step 3. CM creation. Store the number of the first CPs equal to the size of the charged memory (CMS) and their related values of the fitness functions in the charged memory (CM).

*Level 2****: Search***

Step 1. Attracting force determination. Determine the probability of moving each CP toward the others considering the following probability function:

$$p_{ij} = \begin{cases} 1 & \dfrac{fit(i) - fitbest}{fit(j) - fit(i)} > rand \vee fit(j) > fit(i) \\ 0 & \text{otherwise} \end{cases} \tag{34}$$

and calculate the attracting force vector for each CP as follows:

$$\vec{\mathbf{F}}_j = q_i \sum_{i,i\neq j} \left(\frac{q_i}{a^3} \vec{\mathbf{r}}_{ij} . i_1 + \frac{q_i}{\vec{\mathbf{r}}_{ij}^{\,2}} . i_2 \right) P_{ij} (\vec{\mathbf{X}}_i - \vec{\mathbf{X}}_j) \quad \begin{cases} j = 1, 2, ..., N \\ i_1 = 1, i_2 = 0 \Leftrightarrow \vec{\mathbf{r}}_{ij} < a \\ i_1 = 0, i_2 = 1 \Leftrightarrow \vec{\mathbf{r}}_{ij} > a \end{cases} \tag{35}$$

where $\vec{\mathbf{F}}_j$ is the resultant force affecting the *j*th CP.

Step 2. Solution construction. Move each CP to the new position and find its velocity using the following equations:

$$\vec{\mathbf{X}}_{j,new} = rand_{j1} . k_a . \frac{\vec{\mathbf{F}}_{j1}}{m_j} . \Delta t^2 + rand_{j2} . k_v . \vec{\mathbf{v}}_{j,old} . \Delta t + \vec{\mathbf{X}}_{j,old} \tag{36}$$

$$\vec{\mathbf{v}}_{j,new} = \frac{\vec{\mathbf{X}}_{j,new} - \vec{\mathbf{X}}_{j,old}}{\Delta t} \tag{37}$$

where $rand_{j1}$ and $rand_{j2}$ are two random numbers uniformly distributed in the range (1,0); m_j is the mass of the CPs, which is equal to q_j in this paper. The mass concept may be useful for developing a multi-objective CSS. Δt is the time step, and is set to 1. k_a is the acceleration coefficient; k_v is the velocity coefficient to control the influence of the previous velocity. In this paper k_v and k_a are taken as:

$$k_v = c_1 (1 - iter / iter_{\max}), \quad k_a = c_2 (1 + iter / iter_{\max}) \tag{38}$$

where c_1 and c_2 are two constants to control the exploitation and exploration of the algorithm; *iter* is the iteration number and $iter_{\max}$ is the maximum number of iterations.

Step 3. CP position correction. If each CP exits from the allowable search space, correct its position using the HS-based handling as described by Kaveh and Talatahari [18].

Step 4. CP ranking. Evaluate and compare the values of the fitness function for the new CPs; and sort them in an increasing order.

Step 5. CM updating. If some new CP vectors are better than the worst ones in the CM, in terms of their objective function values, include the better vectors in the CM and exclude the worst ones from the CM.

Level 3: Controlling the terminating criterion

Repeat the search level steps until a terminating criterion is satisfied. The CSS algorithm is illustrated in Fig. 2.

For further details and other applications of the CSS, the reader can refer to [30-33].

4. CHARGED SYSTEM SEARCH FOR OPTIMIZING OF TMDS PARAMETERS

In the present work, for analyzing the dynamic response, a general code is written in MATLAB with formulations of the previous sections. Here, we decide to identify all parameters of the TMD consisting of mass, damping and stiffness. For this purpose, according to the previous works, the mass of TMD is taken as a constant, and other parameters are optimized. Optimization process that minimizes the ratio of the maximum story displacements with respect to the ground, are calculated by the developed program due to the El Centro (1940) Earthquake in controlled cases. By addition of the acceleration transfer function (TF) to the objective function, the transmitted force to floors can be controlled due to earthquake ground motion. In general, transfer function is defined as a criterion to evaluate how much of input component is transmitted to the system as a regulated output component. This parameter can be obtained by taking Laplace transform (with zero initial conditions) from state space system defined by Eq. (7) and Eq. (8), and replacing the Laplace transform of Z(t) in Eq. (8) from Eq. (7). Then we have:

$$\mathbf{Y}(s) = (\mathbf{R}(s\mathbf{I} - \mathbf{A})^{-1}\mathbf{B} + \mathbf{Q})\mathbf{F}(s) \tag{39}$$

Transfer function is defined as ratio of the Laplace Transform of regulated output to Laplace transform of the input function (external forces), i.e.

$$T.F = \frac{\mathbf{Y}(s)}{\mathbf{F}(s)} = \mathbf{R}(s\mathbf{I} - \mathbf{A})^{-1}\mathbf{B} + \mathbf{Q} \tag{40}$$

where *T.F* stands for transfer function and other parameters are defined previously. In the case of acceleration transfer function, the matrices **R** and **Q** can be defined as Eq. (13). It should be noted, as seen in Eq. (40), the transfer function is independent of the type of output component and it is considered as an inherent property of system.

In this work, we take the first story as the target, so the objective function can be expressed as [11]:

$$Objective\ \ funtion = \frac{Max\,(controlled\,(x_1))}{Max\,(uncontrolled\,(x_1))} + \frac{Max\,(controlled\,(TF_1))}{Max\,(uncontrolled\,(TF_1))} \tag{41}$$

To apply the CSS to this problem, at each step, the objective function must be calculated for each CP. These are then sorted in the order of their fitnesses. After displacing CPs with Eqs. (28-36), this process is iterated until stopping criterion is satisfied. In this work, the selected parameters of the CSS algorithm are as follows:

$$c_1 = 0.8,\ c_2 = 0.8 \text{ and } \varepsilon = 0.000001$$

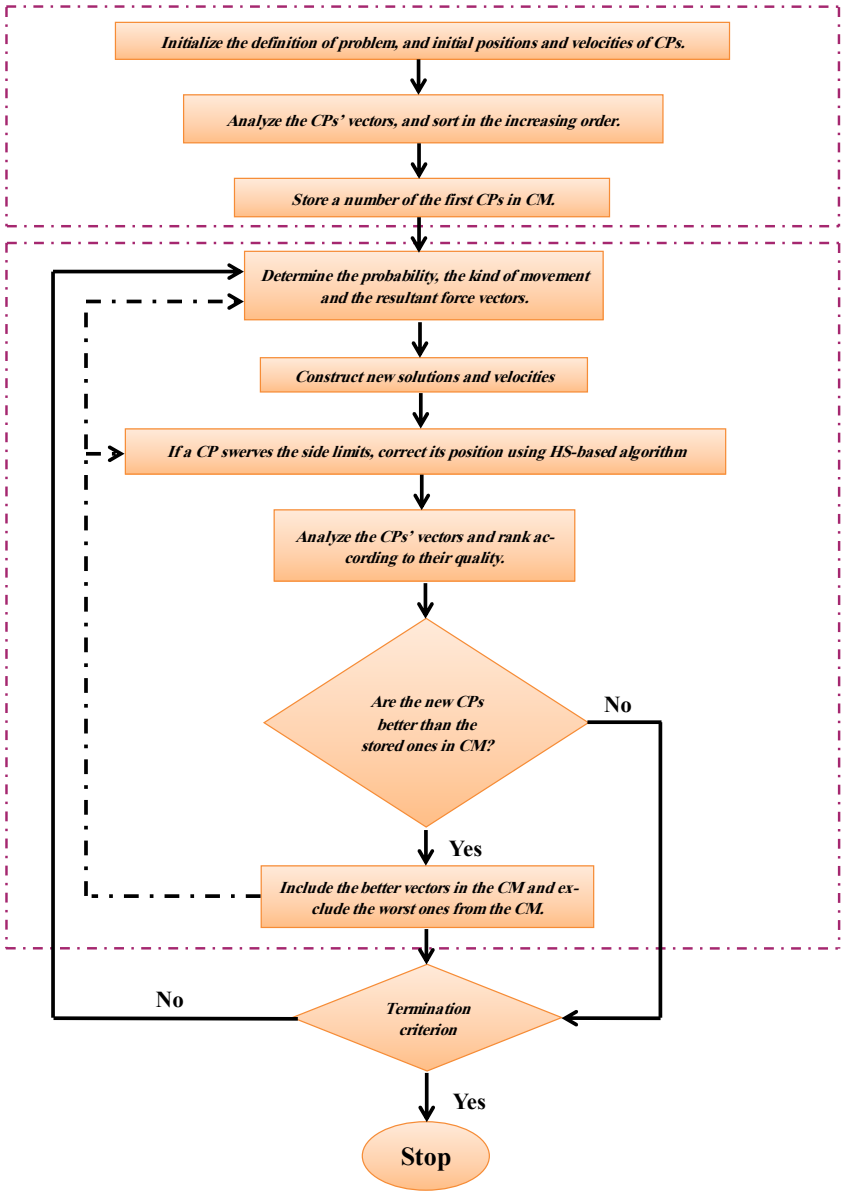

Fig. 2. Flowchart of the charged system search

5. NUMERICAL EXAMPLES

There exist several benchmark examples in literature for comparative studies of the optimization of tuned mass dampers. Here, we have selected two examples and applied the CSS algorithm for optimization of tuned mass dampers, for decreasing the response of the structure. For both examples, the parameters of the CSS algorithm, c_1, c_2, ε, the number of CPs and the number of HMS are taken as 0.8, 0.8, 0.000001, 20 and 5, respectively.

a) Example 1

A ten-story shear building with mass damper attached on the top floor is taken from Hadi and Arfiadi [9]. The properties of building are shown in Table 1.

Table 1. Properties of the building for Example 1

Story	Mass (ton)	Stiffness (kN/m)	Damping (kN.s/m)
1	360	650×10^3	6200
2	360	650×10^3	6200
3	360	650×10^3	6200
4	360	650×10^3	6200
5	360	650×10^3	6200
6	360	650×10^3	6200
7	360	650×10^3	6200
8	360	650×10^3	6200
9	360	650×103	6200
10	360	650×103	6200

In recent works, the mass of TMD were taken constant (m_d=108 ton). In this work, first, we take these the parameters the same as them. Thus the parameters must be selected as design variables in the CSS algorithm which are damping (c_d) and stiffness (k_d) of mass damper. The lower bound and upper bound values of the stiffness are 0 and 5000 kN/m, while the lower bound and upper bound of damping are 0 and 1000 kN-s/m, respectively. After performing the CSS, optimum values for damping and stiffness of TMD are found. Optimum TMD parameters estimated in this paper and the previous works are shown in Table 2. Also, the convergence history of the CSS can be seen in Fig. 3. As it can be observed, the algorithm has converged to optimum solution before 40 iterations (i.e. at 33th iteration).

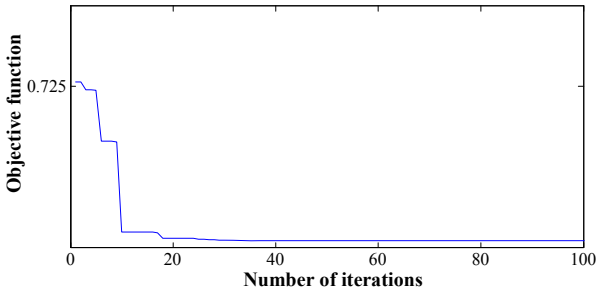

Fig. 3. Variation of the objective function versus the number of iterations for Example 1

Table 2. Stiffness and damping of the TMD for Example 1 (m_d=108 ton)

TMD parameters	Optimum values		
	(GA)[9]	(Lee et al.) [10]	present work(CSS)
$c_d\,(kN-s/m)$	151.5	271.79	88.697
$k_d\,(kN/m)$	3750	4126.93	4207.735

The maximum displacements of each story are presented in Table 3. This table also contains results of the previous works for comparison. Using the present approach, the percentage of reductions in maximum story displacements are between 34.82%–40.23% with mean value of 37.57%. The maximum displacement of first story is reduced to 0.0185 m from 0.031 m (40.23% reduction), and the maximum displacement of the top story is reduced to 0.1225 m from 0.188 m (34.82% reduction). It should be noted that, although the percentage of reduction in some stories is less than those of the other works, the mean value of this parameter is more than that of the other ones. Therefore, one can conclude that the performance of TMD optimized with the present approach, in absorbing seismic energy and reducing total story displacement, is better than those of the previous works. Also, to represent results more comprehensively, the maximum displacements of uncontrolled and controlled structure for all stories are depicted in Fig. 4.

Table 3. Maximum absolute displacement with respect to the ground for El Centro (1940) NS Earthquake

	Maximum absolute displacement with respect to the ground (m)				Percentage of reduction		
	Story	Without TMD	With TMD	With TMD	With TMD		
		(GA)[9]	(Lee et al.) [10]	Present work(CSS)	(GA)	(Lee et al.)	(CSS)
1	0.031	0.019	0.020	0.0185	38.71	35.48	40.32
2	0.060	0.037	0.039	0.0362	38.33	35.00	39.67
3	0.087	0.058	0.057	0.0525	33.33	34.48	39.65
4	0.112	0.068	0.073	0.0682	39.29	34.82	39.11
5	0.133	0.082	0.087	0.0825	38.35	34.59	37.97
6	0.151	0.094	0.099	0.0950	37.75	34.44	37.09
7	0.166	0.104	0.108	0.1056	37.35	34.94	36.39
8	0.177	0.113	0.117	0.1139	36.16	33.90	35.65
9	0.184	0.119	0.123	0.1196	35.33	33.15	35.00
10	0.188	0.122	0.126	0.1225	35.11	32.98	34.84
TMD	-	0.358	0.282	0.4933	mean		
					36.97	34.38	37.57

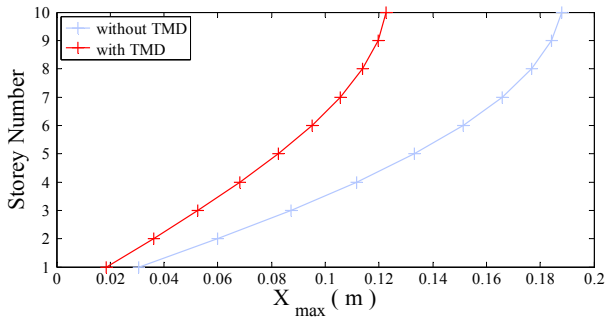

Fig. 4. Maximum displacement for uncontrolled and controlled structure under the El Centro excitation (Example 1, m_d=108 ton)

Additional details of the structural behavior can be obtained by tracking story displacements during the earthquake excitation. To this aim, time history displacement of the first and top floors are plotted in Fig. 5a and Fig. 5b, respectively. Effectiveness of the TMD is also strengthened by the acceleration transfer function defined by Eq. (40). Transfer function graphics for the first and top stories can be seen in Fig. 6c and Fig. 6d.

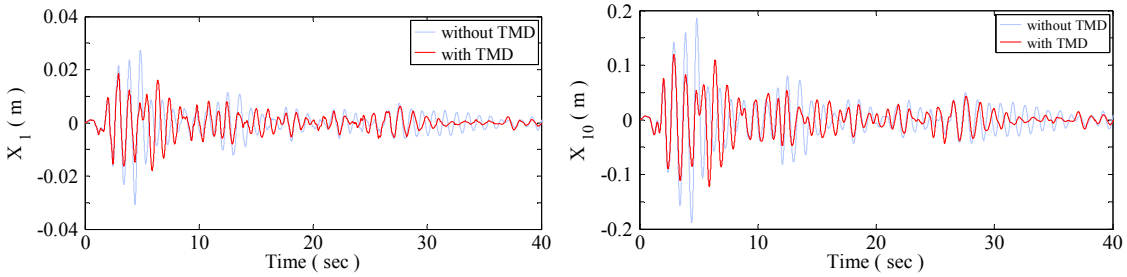

Fig. 5. Time history displacement during the El Centro excitation: (a) first story; (b) top story; (Example 1, m_d=108 ton)

Next we perform the CSS to find the optimum parameters of TMD with different mass varying from 0.02 to 0.04 of total mass of building by step size of 0.0025. The optimum values for each step are shown in Table 4. One can observe from this table that while the value of mass of absorber increases, the corresponding values of optimum damping and stiffness also increase.

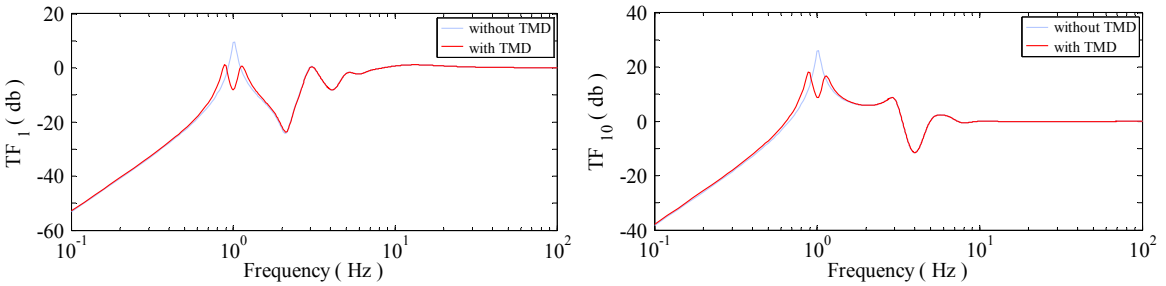

Fig. 6. Transfer function of: (a) first story; (b) top story; (Example 1, m_d=108 ton)

Table 4. Stiffness and damping for different values of the absorber masses (Example 1)

TMD parameters	Optimum value								
Story	m_d (ton)								
	72	81	90	99	108	117	126	135	140
$c_d\,(kN-s/m)$	86.123	76.295	78.644	80.440	88.697	89.282	95.265	99.618	105.034
$k_d\,(kN/m)$	2895.08	3200.4	3513.74	3864.45	4207.73	4478.31	4830.49	5189.39	5379.24

Peak story displacements and the corresponding percent of the reduction for every selected mass are shown in Table 5. It can be revealed from this table that the maximum mean reduction for this case study is obtained by m_d= 99 ton. Although the mean reduction is slightly more than one for the case of m_d= 108 ton, the smaller values for TMD damping and stiffness can support this improvement.

Table 5. Maximum displacements with respect to the ground for El Centro (1940) NS Earthquake for different values of the TMD masses (Example 1)

Story	m_d (ton)								
	72	81	90	99	108	117	126	135	140
1	0.0201	0.0193	0.0191	0.0188	0.0185	0.0192	0.0200	0.0208	0.0209
2	0.0392	0.0378	0.0373	0.0367	0.0362	0.0382	0.0397	0.0413	0.0415
3	0.0568	0.0549	0.0541	0.0533	0.0525	0.0563	0.0586	0.0609	0.0612
4	0.0725	0.0703	0.0693	0.0682	0.0682	0.0733	0.0762	0.0792	0.0797
5	0.0872	0.0841	0.0829	0.0816	0.0825	0.0887	0.0922	0.0958	0.0964
6	0.1002	0.0965	0.0950	0.0935	0.0950	0.1022	0.1062	0.1103	0.1110
7	0.1110	0.1072	0.1056	0.1039	0.1056	0.1136	0.1181	0.1226	0.1234
8	0.1195	0.1159	0.1142	0.1124	0.1139	0.1225	0.1273	0.1322	0.1331
9	0.1254	0.1221	0.1202	0.1184	0.1196	0.1287	0.1338	0.1389	0.1398
10	0.1287	0.1253	0.1234	0.1215	0.1225	0.1318	0.1371	0.1423	0.1433
TMD	0.5158	0.5384	0.5265	0.5172	0.4933	0.4770	0.4583	0.4423	0.4292
	Percent of reduction (%)								
1	35.16	37.74	38.39	39.35	40.32	38.06	35.48	32.9	32.58
2	34.67	37.00	37.83	38.83	39.67	36.33	33.8	31.17	30.83
3	34.71	36.9	37.82	38.74	39.65	35.29	32.64	30.00	29.65
4	35.27	37.23	38.13	39.11	39.11	34.55	31.96	29.29	28.84
5	34.44	36.77	37.67	38.65	37.97	33.31	30.67	27.97	27.52
6	33.64	36.1	37.09	38.08	37.09	32.32	29.67	26.95	26.49
7	33.13	35.42	36.39	37.41	36.39	31.57	28.86	26.14	25.66
8	32.49	34.52	35.48	36.5	35.65	30.79	28.08	25.31	24.81
9	31.85	33.64	34.67	35.65	35.00	30.06	27.28	24.51	24.03
10	31.54	33.35	34.36	35.37	34.84	29.89	27.08	24.31	23.78
mean	33.69	35.87	36.78	37.77	37.57	33.22	30.56	27.86	27.42

Consequently, peak story accelerations and the corresponding percent of reduction are listed for each selected mass in Table 6. Also for better comparison, the data from Table 5 and Table 6 are depicted in Figs. 7a and 7b.

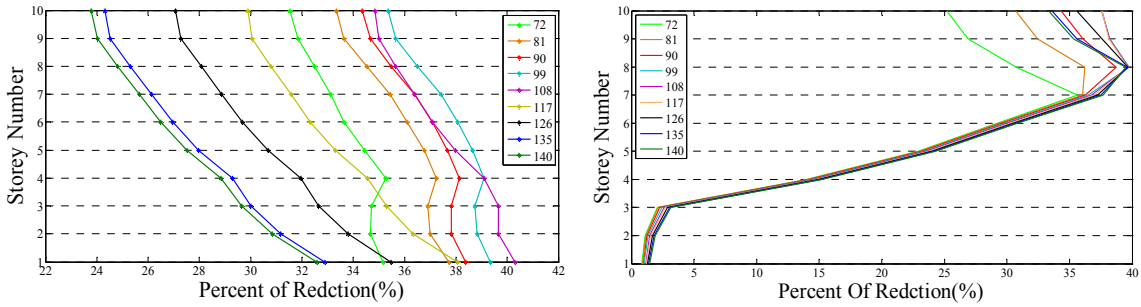

(a) (b)

Fig. 7. Percentage of reduction for: (a) peak story displacements; (b) peak story accelerations; (Example 1)

Table 6. Maximum absolute acceleration with respect to the ground for the El Centro (1940) NS Earthquake for different values of the TMD masses (Example 1)

Story	**Without TMD**	**With TMD**								
		m_d (ton)								
		72	**81**	**90**	**99**	**108**	**117**	**126**	**135**	**140**
1	3.4648	3.4360	3.4348	3.4321	3.4294	3.4260	3.4234	3.4200	3.4168	3.4147
2	5.3378	5.2799	5.2775	5.2720	5.2664	5.2593	5.2542	5.2475	5.2410	5.2367
3	6.133	6.0054	6.0013	5.9929	5.9844	5.9736	5.96579	5.9555	5.9457	5.9393
4	7.3295	6.3066	6.3004	6.2888	6.2771	6.2626	6.2518	6.2380	6.2247	6.2161
5	8.2743	6.3793	6.3704	6.3556	6.3405	6.3223	6.3085	6.2911	6.2742	6.2635
6	8.779	6.2160	6.2038	6.1857	6.1672	6.1456	6.1285	6.1076	6.0872	6.0746
7	9.0516	5.8260	5.7910	5.7697	5.74791	5.7233	5.7030	5.6790	5.6554	5.6411
8	9.2562	6.409	5.9060	5.6721	5.5774	5.5797	5.5837	5.5865	5.5899	5.6032
9	9.4282	6.8909	6.3683	6.0284	5.8250	5.8272	5.8312	5.8825	6.0719	6.0964
10	9.5486	7.1444	6.6148	6.2693	5.9618	5.9564	5.9600	6.1493	6.3394	6.3637
TMD	-	**20.6452**	**21.2485**	**20.5961**	**20.1918**	**19.2500**	**18.4097**	**17.7175**	**17.1403**	**16.6511**
		Percent of reduction (%)								
1	-	0.83	0.869	0.94	1.02	1.12	1.20	1.29	1.39	1.45
2	-	1.09	1.13	1.23	1.34	1.47	1.57	1.69	1.82	1.89
3	-	2.08	2.15	2.28	2.42	2.60	2.73	2.89	3.06	3.16
4	-	13.96	14.04	14.2	14.36	14.56	14.71	14.89	15.08	15.19
5	-	22.91	23.01	23.19	23.37	23.59	23.76	23.97	24.17	24.31
6	-	29.20	29.33	29.54	29.75	30.00	30.20	30.43	30.66	30.81
7	-	35.64	36.02	36.26	36.5	36.77	37.00	37.26	37.52	37.68
8	-	30.76	36.2	38.72	39.74	39.72	39.68	39.65	39.61	39.47
9	-	26.91	32.45	36.06	38.22	38.19	38.15	37.61	35.60	35.34
10	-	25.18	30.73	34.34	37.57	37.62	37.58	35.60	33.61	33.36
mean	-	**18.85**	**20.59**	**21.68**	**22.43**	**22.56**	**22.65**	**22.52**	**22.25**	**22.63**

As mentioned before, the best result for this example is obtained using TMD with properties: m_d= 99 ton, c_d= 80.44 kN.s/m, k_d= 3864.45 kN/m. Further details for this case are shown in Fig. 8 to Fig. 10.

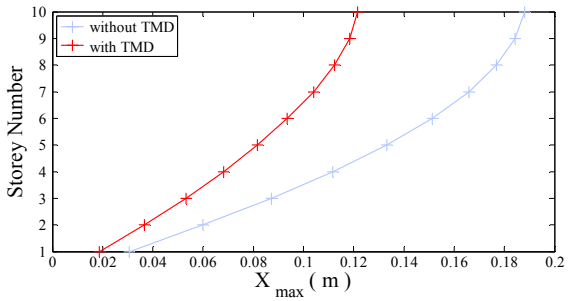

Fig. 8. Maximum displacement for uncontrolled and controlled structure under El Centro excitation (Example 1, m_d=99 ton)

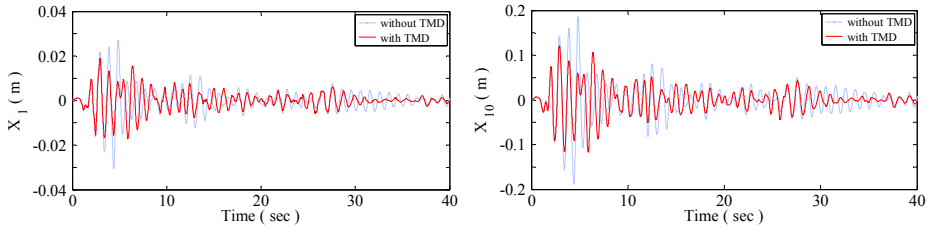

Fig. 9. Time history displacement during the El Centro excitation: (a) first story; (b) top story; (Example 1, m_d=99 ton)

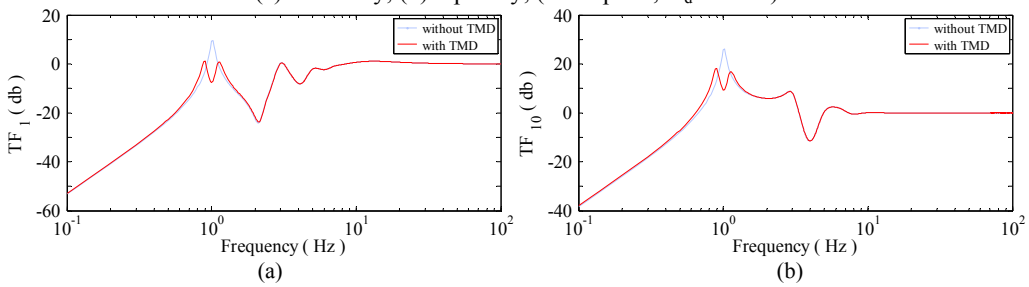

Fig. 10. Acceleration transfer function for: (a) first story; (b) top story; (Example 1, m_d=99 ton)

b) Example 2

The second example has also been investigated by previous researchers, Sadek et al. [8], and Den Hartog [3]. Properties of building are shown in Table 7. For this example, optimum parameters of TMD are obtained as: m_d= 55.45 ton, c_d= 30.234 kN.s/m, and k_d= 355.758 kN/m. These results are significantly smaller than those obtained by Sadek et al. (m_d= 55.45 ton, c_d= 104.4 kN.s/m, and k_d= 464.1 kN/m) [8] and Hadi and Arfiadi (m_d= 55.45 ton, c_d= 48.9 kN.s/m, and k_d= 437.4 kN/m) [9].

Table 7. Properties of the building for Example 2

Story	Mass (ton)	Stiffness (kN/m)	Damping (kN.s/m)
1	179	62470	805.863
2	170	52260	674.154
3	161	56140	724.206
4	152	53020	683.958
5	143	49910	643.839
6	134	46790	603.591
7	125	43670	563.343
8	116	40550	523.095
9	107	37430	482.847
10	98	34310	442.592

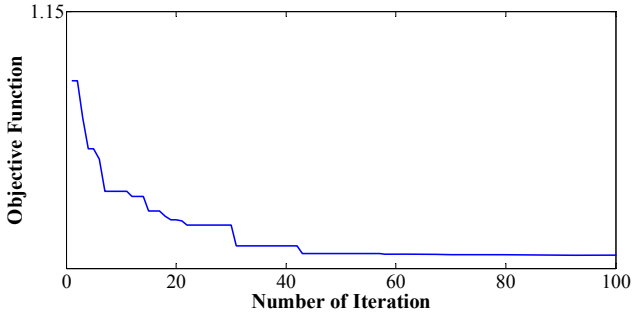

Fig. 11. Variation of the objective function versus the number of iterations for Example 2

The convergence process of the CSS algorithm is shown in Fig. 11. As it can be observed, the algorithm has converged to optimum solution before 100 iterations (i.e. at 86th iteration).

Table 8. Maximum absolute displacement with respect to the ground for the El Centro (1940) NS Earthquake (Example 2)

Story	Without TMD	Den Hartog [3]	Warburton [7]	Sadek et al. [8]	Hadi and Afriadi (GA) [9]	Present work (CSS)
1	0.041	0.034	0.036	0.036	0.034	0.0306
2	0.088	0.074	0.079	0.077	0.072	0.0655
3	0.129	0.106	0.114	0.113	0.105	0.0946
4	0.166	0.136	0.147	0.145	0.134	0.1205
5	0.197	0.163	0.177	0.172	0.160	0.1430
6	0.222	0.187	0.206	0.194	0.184	0.1635
7	0.252	0.213	0.236	0.219	0.210	0.1863
8	0.286	0.239	0.267	0.245	0.236	0.2099
9	0.313	0.261	0.292	0.266	0.258	0.2299
10	0.327	0.276	0.310	0.281	0.272	0.2427
TMD	**-**	**0.602**	**0.751**	**0.456**	**0.635**	**0.6437**
			Percent of reduction (%)			
1	-	17.07	12.20	12.20	17.07	25.37
2	-	15.91	10.23	12.50	18.18	25.56
3	-	17.83	11.63	12.40	18.60	26.67
4	-	18.07	11.45	12.65	19.28	27.40
5	-	17.26	10.15	12.69	18.78	27.41
6	-	15.77	7.21	12.61	17.12	26.35
7	-	15.48	6.35	13.10	16.67	26.06
8	-	16.43	6.64	14.34	17.48	26.61
9	-	16.61	6.71	15.02	17.57	26.54
10	-	15.60	5.20	14.07	16.82	25.78
mean	**-**	**16.60**	**8.78**	**13.16**	**17.76**	**26.37**

The maximum displacements of each story are presented in Table 8. This table also contains results of the previous works for comparison. Using the present approach, the percentage of reductions in maximum story displacements are between 25.37%–27.41% with mean value of 26.37%.

According to Table 8 and Fig. 12, these results are superior to the previous works. The best result after CSS is related to that of Hadi and Afriadi [9] with mean reduction of 17.76%, that is 8.61% less than those of the CSS algorithm.

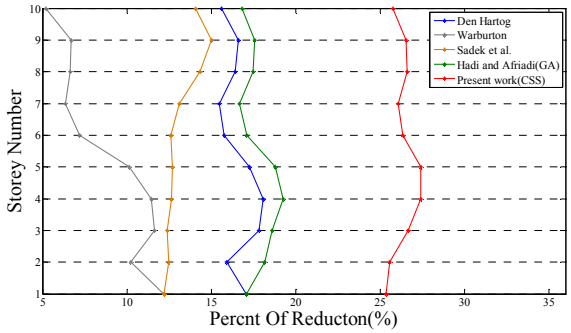

Fig. 12. Percent of reduction for peak story displacements (Example 2).

The maximum displacements of uncontrolled and controlled structure for all stories are depicted in Fig. 13. Further details from structural behavior can be obtained by tracking story displacements during the earthquake excitation. To this aim, time displacement history of the first and top floors are plotted in Fig. 14a and Fig. 14b, respectively.

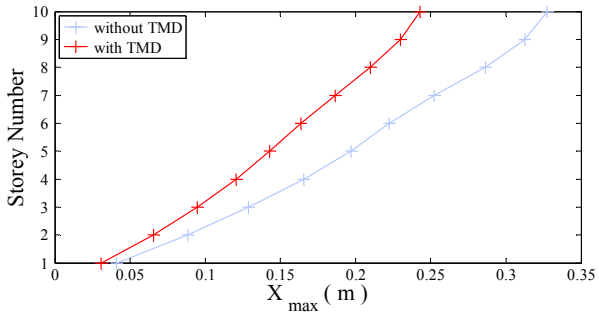

Fig. 13. Maximum displacement for uncontrolled and controlled structure under the El Centro excitation (Example 2)

The effectiveness of the TMD is also strengthened by the acceleration transfer function defined by Eq. (40). Transfer function graphics for the first and top stories can be seen in Figs. 15a and 15b.

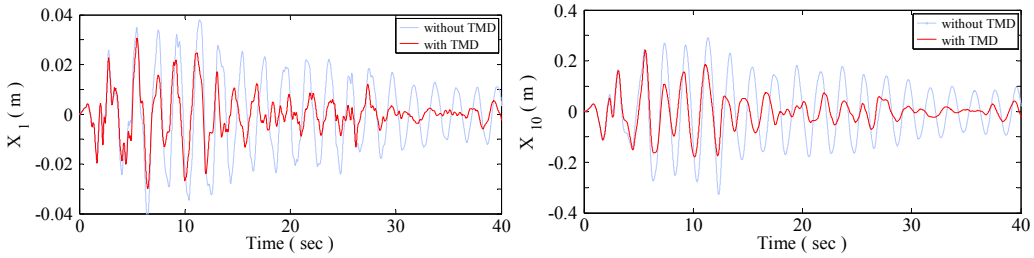

(a) (b)

Fig. 14. Time history displacement during the El Centro excitation: (a) first story; (b) top story; (Example 2)

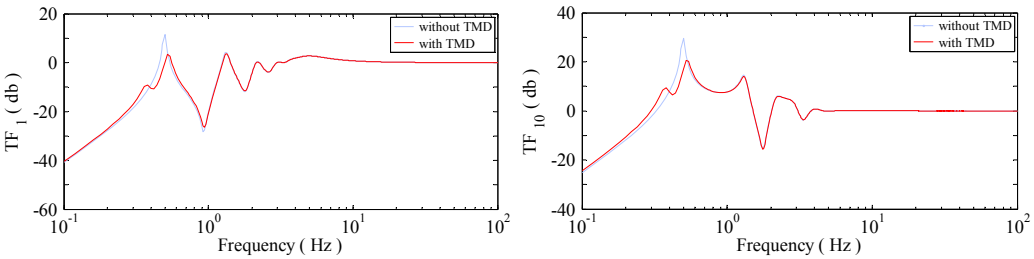

(a) (b)

Fig. 15. Acceleration transfer function for: (a) first story; (b) top story; (Example 2)

c) Computational time

In this work, new formulation is proposed for solving state space equations. Here, the computational time of our Matlab code with the same model is utilized by SIMULINK, Fig. 16. In the Table 9, Average and minimum time for one state-space solution are brought. The results show the superiority of the Matlab code. As can be seen for sine wave loading, the percentage of the reduction of time is about 98%! This reduction for El Centro record is more than 60%. These models are run on a personal computer Core(TM) i7, CPU 2.20GHz, 8.00GB of RAM.

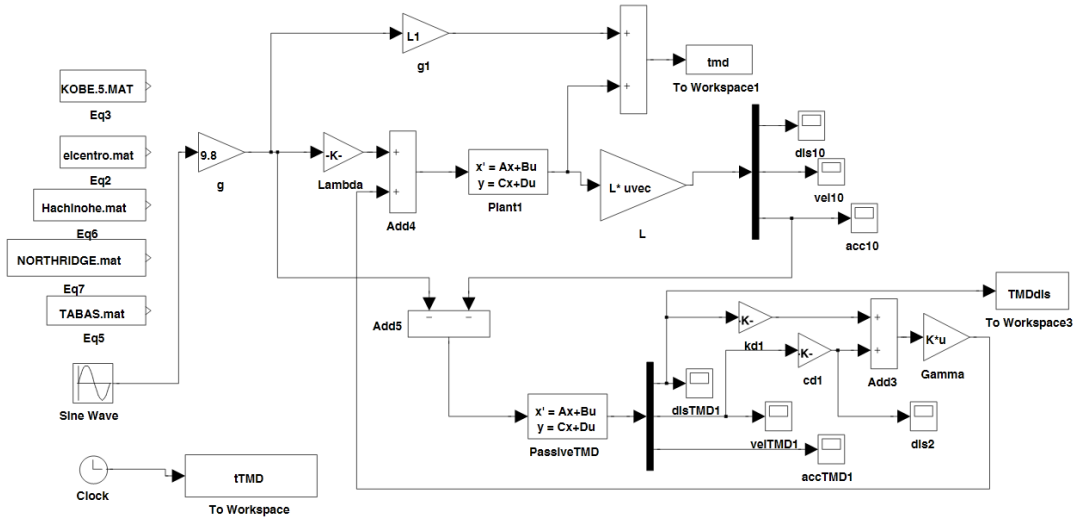

Fig. 16. SIMULINK diagram of the system with TMD

Table 9. Average and minimum time comaparison of two models

	Time (Sec.)	Matlab code	SIMULINK Model
Sine wave	**Average**	0.0283	1.3791
	Min	0.0221	1.3560
El centro	**Average**	0.6014	1.4937
	Min	0.5765	1.4702

6. CONCLUSION

The overall objective of this paper was to determine the optimum parameters of tuned mass dampers that result in utmost reduction in the structural response to earthquake loading. Charged system search, a well operation optimization algorithm in engineering problems, is used to estimate optimum parameters of TMD. The objective function used in this study is based on that of reference [11]. In order to solve equations of motion in state space form, an alternative procedure is utilized which is based on matrix exponential approach. The present formulation is general and can be used to find the response of all mechanical systems subjected to any external excitation. However, to make the results comparable with the previous works, the assembling procedure of mass, stiffness, and damping matrices of the system were defined only for the case of shear frames with one translational degree of freedom on each story level. For 3-D or irregular structures, the formulation should be modified properly.

To verify the capability of the present optimization procedure, some numerical calculations are performed on two well established examples.

In the first example, a ten-story shear building is considered. It is found that with the same damper mass, the mean value of displacement reduction is 37.57% which is more than those of the previous studies. It means more capability in absorbing earthquake energy and reducing total story displacements is achieved in this work. Also, in the next step more refinement is applied on the mass of TMD. In this step, it is found that better solution can be obtained by smaller values of TMD parameters (m_d = 99 ton, c_d = 80.441 kN.s/m, and k_d = 3864.45 kN/m). In this case, the maximum top story displacement is reduced to 0.1215 m from 0.188 m (35.37% reduction), and the mean value of the reduction is 37.77%. Although the mean displacement reduction is slightly more than one for the case of m_d= 108 ton, smaller values for TMD damping and stiffness can support this improvement. The other fact that can be concluded from this refinement is that decreasing the value of TMD mass will be followed with decreasing in other parameters of TMD (stiffness and damping). On the other hand, with the smaller value of TMD mass the reduction on story displacements becomes more uniform. Also, it is observed that sensitivity of acceleration reduction with TMD mass is negligible except on the three upper floors.

In the second example, we were only interested in finding the optimum value of the TMD parameters and the corresponding reduction in displacement values. In this case, optimum parameters of TMD are obtained as: m_d = 55.45 ton, c_d = 30.234 kN.s/m, and k_d= 355.758 kN/m. These optimum values are significantly smaller than those obtained by Sadek et al. [8] and Hadi and Arfiadi [9]. Also, displacement reduction of this case for the present study are superior to the previous works, as the best result after the present work is related to Hadi and Afriadi [9] with mean reduction of 17.76%, that is 8.61% less than those of the present study.

REFERENCES

1. Frahm, H. (1911). *Device for damping of bodies*, U.S. Patent, No. 989958.
2. Ormondroyd, J. & Den Hartog, J. P. The theory of dynamic vibration absorber. *Transactions of the American Society of Mechanical Engineers*. Vol. 50, pp. 9–22.
3. Den Hartog, J. P. (1956). *Mechanical Vibrations*. McGraw-Hill.
4. McNamara, R. J. (1977). Tuned mass dampers for buildings. *Journal of the Structural Division. ASCE.* Vol. 103, pp. 1785-1798.
5. Luft, R. W. (1979) Optimum tuned mass dampers for buildings. *Journal of the Structural Division. ASCE*. Vol. 105, pp. 2766-2772.
6. Falcon, K. C., Stone, B. J., Simcock, W. D. & Andrew, C. (1967). Optimization of vibration absorbers: A graphical method for use on idealized systems with restricted damping. *Journal of Mechanical Engineering Science*. Vol. 9, pp. 374-381.
7. Warburton, G. B. (1982). Optimum absorber parameters for various combinations of response and excitation parameters. *Earthquake Engineering and Structural Dynamics*. Vol. 10, pp. 381–401.
8. Sadek, F., Mohraz, B., Taylor, A. W. & Chung, R. M. (1997). A method of estimating the parameters of tunedmass dampers for seismic applications, *Earthquake Engineering and Structural Dynamics*. Vol. 26, pp. 617–635.
9. Hadi. M. N. S. & Arfiadi, Y. (1998). Optimum design of absorber for MDOF structures. *Journal of the Structural Division. ASCE*. Vol. 124, pp. 1272–1280.
10. Lee, C. L., Chen, Y. T., Chung, L. L. & Wang, Y. P. (2006). Optimal design theories and applications of tuned mass dampers. *Engineering Structures*. Vol. 28, pp. 43–53.
11. Bekdas, G. & Nigdeli, S. M. (2011). Estimating optimum parameters of tuned mass dampers using harmony search. *Engineering Structures*. Vol. 33, pp. 2716–2723.

12. Miguel, L. F. Fadel, Lopez, R. F. & Miguel, L. F. F. (2013). Discussion of paper: Estimating optimum parameters of tuned mass dampers using harmony search. *Engineering Structures*. Vol. 54, pp. 262–264.
13. Bekdas, G. & Nigdeli, S. M. (2013). Response of discussion on Estimating optimum parameters of tuned mass dampers using harmony search. *Engineering Structures*. Vol. 54, pp. 265–267.
14. Kaveh, A. & Kalatjari, V. (2004). Size/geometry optimization of trusses by the force method and genetic algorithm. *ZAMM Journal of Applied Mathematics and Mechanics.* Vol. 84, pp. 347–357.
15. Li, L. J., Huang, Z. B., Liu, F. & Wu, Q. H. (2007). A heuristic particle swarm optimizer for optimization of pin connected structures. *Computers & Structures.* Vol. 85, pp. 340–349.
16. Kaveh, A. & Shojaee, S. (2007). Optimal design of skeletal structures using ant colony optimization. *International Journal for Numerical Methods in Engineering.* Vol. 70, pp. 563–581.
17. Lee, K. S. & Geem, Z. W. (2004). A new structural optimization method based on the harmony search algorithm. *Computers & Structures*. Vol. 82, pp. 781–798.
18. Kaveh, A. & Talatahari, S. (2010). A novel heuristic optimization method: charged system search. *Acta Mechanica.* Vol. 213, pp. 267-289.
19. Kaveh, A. & Talatahari, S. (2010). Optimal design of skeletal structures via the charged system search algorithm. *Structural and Multidisciplinary Optimization*. Vol. 41, pp. 893-911.
20. Singh, M. P., Singh, S. & Moreschi, L. M. (2002). Tuned mass dampers for response control of torsional buildings. *Earthquake Engineering and Structural Dynamics*. Vol. 31, pp. 749–769.
21. Marano, G. C., Greco, R. & Chiaia, B. (2010). A comparison between different optimization criteria for tuned mass dampers design. *Journal of Sound and Vibration*. Vol. 329, pp. 4880–4890.
22. Steinbuch, R. (2011). Bionic optimisation of the earthquake resistance of high buildings by tuned mass dampers. *Journal of Bionic Engineering*. Vol. 8, pp. 335-344.
23. Leung, A.Y.T. & Zhang, H. (2009). Particle swarm optimization of tuned mass dampers. *Engineering Structures*. Vol. 31, pp. 715–728.
24. Bekdas, G. & Nigdeli, S. M. (2011). Investigation of SDOF idealization for structures with optimum tuned mass dampers. *Proceedings of the Natural Cataclysms and Global Problems of the Modern Civilization Geocataclysms, Istanbul, Turkey.*
25. Bekdas, G. & Nigdeli, S. M. (2011). Optimization of tuned mass damper parameters for structures subjected to earthquakes with forward directivity. *Proceedings of the Natural Cataclysms and Global Problems of the Modern Civilization Geocataclysms, Istanbul, Turkey.*
26. Bekdaş, G. & Nigdeli S. M. (2013). Mass ratio factor for optimum tuned mass damper strategies. *International Journal of Mechanical Science*. Vol. 71, pp. 68–84.
27. Farshidianfar, A. & Soheili, S. (2013). Ant colony optimization of tuned mass dampers for earthquake oscillations of high-rise structures including soil-structure interaction. *Soil Dynamic and Earthquake Engineering*. Vol. 51, pp. 14–22.
28. Islam, B. & Ahsan, R. (2012). Optimization of tuned mass damper parameters using evolutionary operation algorithm. *15th World Conference in Earthquake Engineering (WCEE), Lisbon, Portugal*.
29. Fairman, F. W. (1998). *Linear Control Theory, The State Space Approach*. John Wiley and Sons, Chichester, New York, Weinheim, Brisbane, Singapore, Toronto.
30. Kaveh, A. (2014). *Advances in Metaheuristic Algorithms for Optimal Design of Structures*, Springer Verlag, Wien.
31. Kaveh, A. & Sharafi, P. (2012). Ordering for bandwidth and profile minimization problems via charged system search method, *Iranian Journal of Science and Technology, Transactions of Civil Engineering*, Vol. 36, pp. 39-52.

32. Kaveh, A., Talatahari, S. & Farhmand Azar, B. (2012). Optimum design of composite open channels using charged system search algorithm, *Iranian Journal of Science and Technology*, *Transactions of Civil Engineering*, Vol. 36, pp. 67-77.
33. Kaveh, A. Massoudi, M. S. & Ghanooni Bagha, M. (2014). Structural Reliability Analysis Using Charged System Search Algorithm, *Iranian Journal of Science and Technology*. *Transactions of Civil Engineering*, Vol. 38, No. C2, pp. 439-448.